

CRITICAL EVALUATION OF CORN SILO BURST FAILURE ANALYSIS

MTRL 585 Case Study 3

Prepared By:
GROUP 7

Janna Fabris



Wade Gubbels



Ibrahim Gadala



Darren Bromley



Submitted 16 October 2012

Contents

List of Figures.....	3
List of Tables.....	3
1.0 INTRODUCTION.....	4
2.0 FACTS AND EVENTS	4
2.1 Background.....	4
2.1 Post-accident investigations and failure hypothesis	4
2.2 Experimental Investigations.....	5
2.2.1 Tensile test	5
2.2.2 Metallographic analysis	5
3.0 ENGINEERING ANALYSIS	6
3.1 Strength analysis	6
3.2 Fracture mechanics	9
4.0 CRITICAL EVALUATION	13
4.1 Relevance of facts presented	13
4.2 Missing information	13
4.3 Appropriateness of analysis presented.....	14
4.4 Failure prevention	15
4.5 General comments	16
5.0 CONCLUSION.....	17
REFERENCES.....	18

List of Figures

Figure 1: Variation in hydrostatic pressure through height of silo	8
--	---

List of Tables

Table 1: Details of burst silo	4
Table 2: Average St37-3N mechanical property results from tensile test.....	5
Table 3: Calculated hoop stresses in static and dynamic loading conditions.....	7
Table 4: Properties and stresses calculated for barley and corn	9
Table 5: Crack lengths for stable crack extension and unstable crack propagation under static load for different sheet conditions (thicknesses)	11
Table 6: Sensitivity analysis of stress level and dynamic fracture toughness factors	12

1.0 INTRODUCTION

Authors G. Piskoty, S.A. Michel and M. Zraggen present an interdisciplinary failure analysis to identify and assess, experimentally and theoretically, the probable cause of a corn silo burst [1]. The approach adopted by the authors was critically evaluated to understand key engineering principles and the failure analysis techniques used.

2.0 FACTS AND EVENTS

2.1 Background

A 16 year old silo structurally failed during standard operation, as per the following sequence of events:

- initially fully filled with corn (approximately 700 tonne)
- emptying process commences (approximately 15 tonnes is released)
- the process is interrupted by a visual inspection
- silo catastrophically bursts suddenly thereafter

Details of the burst silo are summarized in Table 1.

Table 1: Details of burst silo

contents of silo	grain: barley / corn
construction	St37-3N corrugated sheet metal 18 sheets ("rings") screwed to 36 vertical metal stiffeners U-shaped vertical stiffeners are secured to concrete foundation with anchor bolts
corrosion protection	sheet metal galvanized with zinc layer on both sides
ventilation	internal airflow cooling system contents of silo cooled to 15°C
dimensions	h = 17m D = 8m t = 7.0E-4m

2.1 Post-accident investigations and failure hypothesis

The authors gathered background information from several sources, including:

- a visual inspection of the accident site
- statements from witnesses and police

Additionally, a root-cause analysis was conducted to identify possible causes of failure (failure hypotheses). This information revealed several irregularities with which the authors were able to make an informed engineering decision regarding

the probable cause of the silo burst. It was concluded that the likely root cause of failure was due to a “main crack” in an area of the sheet metal weakened by corrosion. This hypothesis was subject to further investigation to determine whether:

- the sheet-metal was overloaded in the corroded area
- in validating the crack assumption, did a probable initial crack length exceed a critical crack length

The authors confirmed this hypothesis by:

- experimental test
 - tensile testing: material characterization and identification
 - metallographic examination of the failed material
- theoretical analysis
 - strength analysis: silo’s likely stress state at time of accident
 - fracture mechanics assessment: determination of unstable crack growth

2.2 Experimental Investigations

2.2.1 Tensile test

Tensile tests of non-corroded section of sheet-metal were conducted, as per standard EN 10’002-1. The key averaged mechanical properties obtained from these tests are summarized in Table 2. The authors were able to deduce that this material was St37-3N, a low-alloyed steel typically used in the construction of grain silos.

Table 2: Average St37-3N mechanical property results from tensile test

yield strength	R _{p0.2}	MPa	297
ultimate strength	R _m	MPa	386
fracture elongation	A ₅₀	%	30.9

2.2.2 Metallographic analysis

In addition to the identification of the failed material, the authors employed metallographic analysis to examine the microstructure and wall thickness of non-corroded and corroded sections of sheet-metal. The images shown in their report, Figures 10 and 11, clearly show the galvanic zinc layer and the ferritic-perlitic microstructure of the steel.

The authors confirmed that due to corrosion attack, the residual wall thickness was reduced by up to 56% in the corroded sections analyzed.

3.0 ENGINEERING ANALYSIS

3.1 Strength analysis

In their strength analysis, the authors decided to only consider the effect of hydrostatic pressure of the corn. Relevant parameters were provided as follows:

- Diameter of the silo $D = 8 \text{ m}$
- Ultimate strength of the sheet metal $R_m = 386 \text{ MPa}$
- Corn column above corroded area $z = 13 \text{ m}$
- Density of the corn $\gamma = 8 \text{ kN/m}^3$
- Horizontal load ratio $\lambda = 0.65$
- Wall friction for rough walls $\mu = 0.5$
- Nominal thickness of the sheet $t_n = 0.7 \text{ mm}$
- Thickness of the corroded sheet $t_{cor} = 0.3 - 0.4 \text{ mm}$
- Dynamic load factor for corn releasing process $e_h = 1.4$

According to DIN standard 1055, the hydrostatic pressure of the corn is calculated according to the following equations. The authors' results were confirmed, as p_{hyd} was determined to be 28.1 kPa.

$$p_{hyd} = \frac{\gamma D}{4\mu} (1 - e^{-z/z_0})$$

$$z_0 = \frac{D}{4\lambda\mu}$$

The circumferential tensile stress in the silo walls (hoop stress) was calculated as a function of hydrostatic pressure in both static (σ_{st}) and dynamic (σ_{dyn}) cases according to the following equations:

$$\sigma_{st} = \frac{p_{hyd} D}{2t}$$

$$\sigma_{dyn} = e_h \sigma_{st}$$

Stresses were calculated in the case of the un-corroded sheet, and at locations of maximum, minimum, and average corroded area thicknesses. Table 3 shows that dynamic hoop stress calculated with the design load factor of 1.4 exceeds the measured yield strength of 297 MPa in all corroded areas. Stresses were also evaluated using a load factor of 1.2, which was calculated from a ratio of ultimate tensile strength to static stress at average corroded thickness (i.e. $e_h = 386/322$). It was not useful of the authors to state that “even” with a load factor of 1.2, failure would be encountered, since the load factor was calculated from the failure criterion itself. Rather, it could have been stated that the surfaces of average corrosion would only suit a design with a dynamic load factor of 1.2.

Neglecting the effect of stress concentrators, the corrosion tolerance could have been determined. In static loading conditions, failure would be initiated in a wall corroded 58% through the thickness, and in dynamic loading conditions (assuming a loading factor of 1.4), failure would be initiated in a wall corroded only 42% through the thickness.

Table 3: Calculated hoop stresses in static and dynamic loading conditions

Condition	t (mm)	σ_{st} (MPa)	$\sigma_{dyn,1.4}$ (MPa)	$\sigma_{dyn,1.2}$ (MPa)
Original sheet (un-corroded)	0.7	161	225	193
Corroded sheet, max thickness	0.4	281	394	338
Corroded sheet, min thickness	0.3	375	525	450
Corroded sheet, average thickness	0.35	321	450	386

To gain an appreciation for the variation across the height of the silo, hydrostatic pressure and hoop stresses in an un-corroded sheet were calculated as a function of distance from the top of the corn (Figure 1). Considering only hydrostatic pressure, the silo walls would be able to withstand hoop stresses in the un-corroded condition.

In the analysis, the authors make no mention of the effect of having corrugated versus flat silo walls. This will have an impact on horizontal forces from hydrostatic pressure, friction at the walls, and vertical loading of the walls; all of which are a function of the effective friction. Details of the corrugation are not provided in the report, but DIN 1055 provides assistance in Section D.2. The following equation is used to determine the effective friction, μ_{eff} :

$$\mu_{eff} = (1 - a_w) \tan \varphi_i + a_w \mu_w$$

The authors inconsistently and interchangeably refer to the material contained within the silo as either corn or barley. Although the properties are similar, this is believed to be an oversight easily avoided. For example, differences in the angle of internal friction (φ_i) and the coefficient of wall friction (μ_w) result in a variance of 12.5% with respect to effective friction in a corrugated silo wall (μ_{eff}). Since the title of the paper refers to corn, we believe that the term barley was used in error.

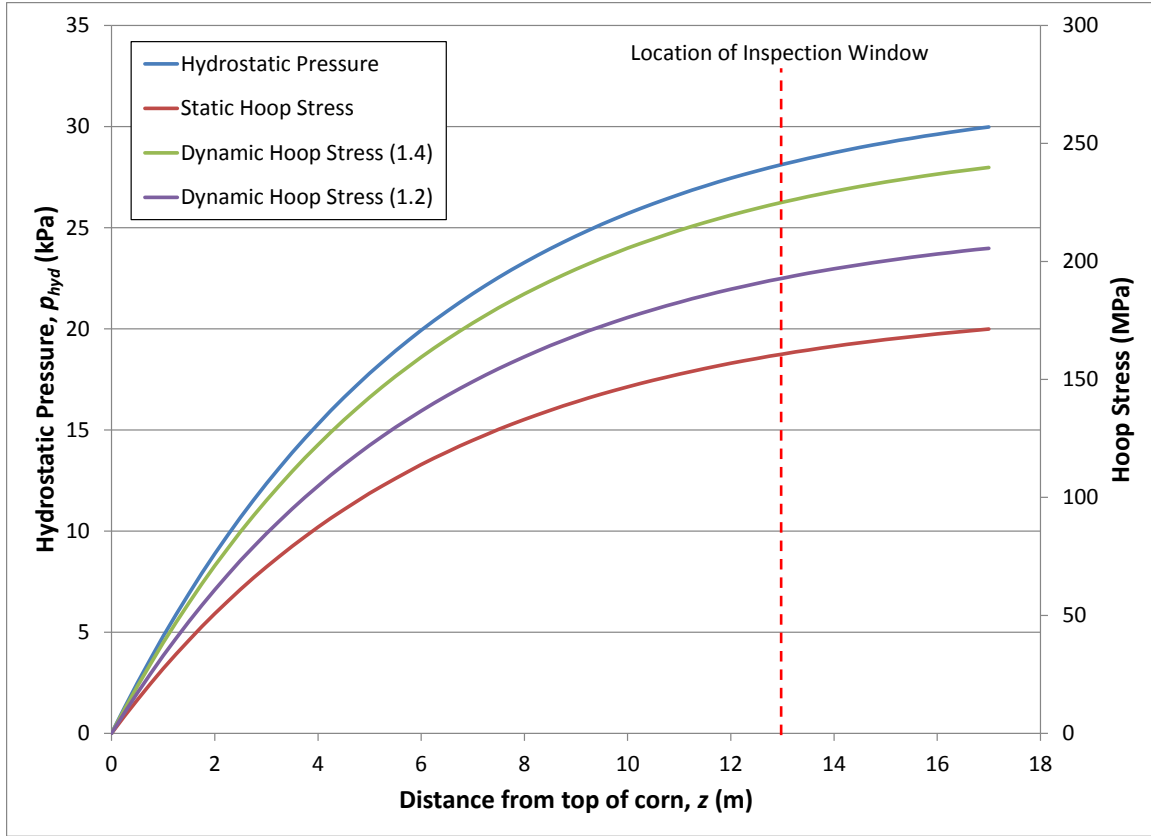


Figure 1: Variation in hydrostatic pressure through height of silo

As per DIN 1055, the silo involved in the incident classifies as a slim silo (height is greater than 2 times the diameter). According to Section 7.2.1.1, stresses due to friction and vertical loading can be determined from the following equations:

$$p_{fric} = \frac{\gamma D}{4} (1 - e^{-z/z_0})$$

$$p_{vert} = \frac{\gamma D}{4\lambda\mu} (1 - e^{-z/z_0})$$

For a corrugation wall with a sinusoidal profile (as it appears from the pictures in the report), DIN 1055 provides an estimate for a_w of 0.2. Properties for rough walls and calculated stress for both barley and corn at the inspection window are shown in Table 4. It is shown here that in neglecting the effect of corrugation, the hydrostatic pressure was overestimated by the authors by approximately 12%, assuming that the silo contained corn rather than barley. On the other hand, the calculations confirm validity of the authors' assumption to neglect the vertical loads.

Table 4: Properties and stresses calculated for barley and corn

Property	Corn	Barley
φ_i	31°	28°
μ_w	0.53	0.48
μ_{eff}	0.59	0.52
p_{hyd} (kPa)	25.0	27.3
p_{fric} (kPa)	14.7	14.2
p_{vert} (kPa)	38.4	42.0

3.2 Fracture mechanics

In the fracture mechanics assessment, the authors' goal was to estimate the critical crack length in the sheet in the corroded area and the non-corroded area, using the corresponding stresses found using the stress analysis. Their main simplification was the use of linear-elastic fracture mechanics equations and concepts. We disagree with the suitability of this simplification, due to the size of the plastic zone compared to the thickness of the material. This concern will be addressed in the subsequent critical evaluation segment. However, due to the complexity of elastic-plastic fracture mechanics, we do not attempt to do such an analysis for comparison. In this section, we simply recreate the authors' analysis, while commenting and critiquing the suitability of their assumptions and methods.

In the analysis, the fracture mechanics parameters for St37-3N steel were used, after the tensile test results revealed the mechanical performance of the actual silo steel being very similar. From reference [2] (in the article), the fracture mechanics parameters reported were:

- the J-integral
- the crack extension δ values at the initiation of stable crack extension
- the notch bar impact value (KV) at room temperature

$$J_i = 145 \text{ N/mm} \quad \delta_i = 0.24 \text{ mm} \quad KV = 160 \text{ J}$$

The authors then assumed small-scale yielding (which is again, invalid) to find the stress intensity factor for stable crack extension:

$$K_i = \sqrt{J_i \cdot E}$$

With the literature value for $E = 210 \text{ GPa}$, the value for $K_i = 174 \text{ MPa}\sqrt{\text{m}}$.

For unstable crack propagation, the stress intensity factor $K_{j(\Delta a)}$ is estimated based on the equation from the reference [2] (in the article) which includes KV and the stable crack extension Δa , calculated for the plane strain condition:

$$K_{j(\Delta a)} = \sqrt{\frac{E}{1-\nu^2} \cdot \frac{0.53 \cdot KV^{1.28} \cdot \Delta a^{0.133 \cdot KV^{0.256}}}{1000}} \text{ MPa}\sqrt{\text{m}}$$

However, the stress condition of the silo sheet was previously simplified to plane stress, and rightly so due to the presence of negligible out-of-plane stresses compared to in-plane. Thus, the $\frac{E}{1-\nu^2}$ term is substituted by E . The authors also substitute the stable crack extension term Δa with the crack extension term δ at the initiation of stable crack extension. Although δ represents the stable crack extension term at crack initiation, this substitution is reasonable given the small effect Δa has on the final results.

The critical stress intensity factor for unstable crack propagation in the plane stress condition now becomes:

$$K'_{j(\Delta a)} = \sqrt{E \cdot \frac{0.53 \cdot KV^{1.28} \cdot \delta_i^{0.133 \cdot KV^{0.256}}}{1000}} = 192 \text{ MPa}\sqrt{\text{m}}$$

The stable and unstable critical stress intensity factors were substituted into the basic equation for fracture mechanics ($K = \sigma \cdot \sqrt{\pi \cdot a} \cdot Y$). Again, the use of this equation in its basic form is correct only if LEFM is valid. The crack lengths for stable (l_i) and unstable (l_c) crack propagation are two times the crack length a , because the crack geometry was a through-crack type. Also, a geometry factor $Y = 1$ was used since the through crack geometry was considered to be in an infinite wide thin plate under uniform tension. Although we agree with this crack geometry simplification, we think the authors neglected the fact that vertical stresses do occur in the wall due to the friction between the contents of the silo and the inner wall, causing shear stresses. This stress can be assumed to be negligible (as indicated in the strength analysis of section 3.1), but, for thoroughness, it should have been mentioned.

$$l_i = 2 \cdot a_i = 2 \cdot \frac{\left(\frac{K_i}{\sigma}\right)^2}{\pi} \quad l_c = 2 \cdot a_c = 2 \cdot \frac{\left(\frac{K'_{j(\Delta a)}}{\sigma}\right)^2}{\pi}$$

Using the static stress values from Table 3, the resultant crack lengths are summarized in Table 5.

Table 5 reveals that for any thickness condition in the corroded area, the critical crack lengths calculated are less than the vertical spread observed at the corroded zone ($c \approx 300 \text{ mm}$). Thus, for the actual spread of the corroded zone, $K > K_c$ and unstable crack propagation is explainable even under static load.

However, Table 5 also reveals that the critical crack lengths for stable crack extension or unstable crack propagation are much larger in the non-corroded or original sheet than the actual crack length at failure. The authors present an explanation as to why the crack did not stop when it encountered the original sheet thickness area (the border of the corroded region).

The two reasons provided were:

- Interrupting the emptying process caused sliding of the silo contents which increased the load level ($\sigma > \sigma_{st}$).
- Lower fracture toughness value for dynamic scenarios as opposed to static scenarios. This case was dynamic since the crack was “in motion” as it reached the non-corroded zone ($K_d < K_c$).

Table 5: Crack lengths for stable crack extension and unstable crack propagation under static load for different sheet conditions (thicknesses)

	Corresponding stress intensity factor K (MPa \sqrt{m})	Crack length l (mm)			
		Original sheet (uncorroded) $\sigma_{st} = 161$ MPa	Corroded sheet (average thickness) $\sigma_{st} = 321$ MPa	Corroded sheet (max thickness) $\sigma_{st} = 281$ MPa	Corroded sheet (min thickness) $\sigma_{st} = 375$ MPa
Stable crack extension	$K_i = 174$	$l_{non,i} = 744$	$l_{cor-av,i} = 187$	$l_{cor-max,i} = 244$	$l_{cor-min,i} = 137$
Unstable crack propagation	$K_{j(\Delta a)} = 192$	$l_{non,c} = 905$	$l_{cor-av,c} = 228$	$l_{cor-max,c} = 297$	$l_{cor-min,c} = 167$

Although our group agrees with the difference these two points make, we believe the subsequent assumptions for the “post-sliding” stress level and the dynamic fracture toughness to be haphazard. The authors assume the “post-sliding” stress level as 1.4 times the static stress level (same as dynamic stress in the strength analysis), and the dynamic fracture toughness as 0.8 times the critical unstable crack propagation stress intensity factor $K'_{j(\Delta a)}$. We think that the “post-sliding” stress increase should not be as severe as the dynamic stress, and since the failure did not occur *during* a filling or emptying process, using such a value can lead to an incorrect conclusion. In addition, no explanation or reference was given for the use of 0.8 as the dynamic fracture toughness factor. To assess the effect these values have on the resulting critical length values, our group did a preliminary sensitivity analysis. Table 6 outlines this analysis, where the left edge column represents different values for “post-sliding” stress level, the top column represented different dynamic fracture toughness factor values, and the cells in between represent corresponding critical crack lengths $l_{non,c,dyn}$. The red indicates values which would cause continuation of the crack through the non-corroded zone and the green indicated crack length values which would have been arrested. The white values are those which are very close to the corroded area spread (≈ 300 mm).

As seen in the sensitivity analysis below, the critical crack length of approximately 300 mm can be achieved with multiple variations of stress factors and dynamic fracture toughness factors. In addition, with only slight changes in any of the two factors (like changing the stress factor to 1.2 instead of 1.4, keeping the dynamic factor the same at 0.8), crack length values which invalidate the authors' conclusion can be calculated. Thus, our group found it very important for the authors to back up the use of the factors in the paper by indicating a literature source where they come from or, at least, mentioning that sensitivity of calculated crack lengths with respect to these factors is high.

Table 6: Sensitivity analysis of stress level and dynamic fracture toughness factors

	Dynamic K factor	0.95	0.9	0.85	0.8	0.75	0.7
Stress factor							
1.1		675	606	541	479	421	367
1.2		567	509	454	402	354	308
1.3		483	434	387	343	301	263
1.4		417	374	334	296	260	226
1.5		363	326	291	258	226	197
1.6		319	286	256	226	199	173

The authors calculate the size of the plastic zone in order to assess the legitimacy of using LEFM for the analysis. The plane stress condition plastic zone size is estimated by:

$$\omega = \frac{1}{2.05 \cdot \pi} \cdot \frac{K_{max}}{\sigma_s^2}$$

Using the average of $K_{j(\Delta a)}$ and $K'_{j(\Delta a)}$ for K_{max} , and the average of $R_{p0.2}$ and R_m from the tensile tests for σ_s , the plastic zone size was found to be 44 mm. The authors then claim that because this value is “small enough” compared to the average critical length of the corroded zone ($\frac{l_{cor-av,i} + l_{cor-av,c}}{2} \approx 200$ mm), small scale yielding occurs and LEFM use is justified. We disagree with this, as will be discussed in the subsequent critical analysis. Briefly put, the ratio of plastic size to crack length using these numbers is actually quite significant ($> 20\%$), which is not normally considered to be small enough for small scale yielding (usually 5% or less). Furthermore, the plastic zone size is much larger than the thickness of the sheet, even in the original non-corroded condition. LEFM should not be used in such cases. That being said though, a large plastic zone compared to sheet thickness does indeed justify plane stress assumption, since plasticity increases with decreased thickness. This is mentioned correctly in the paper.

4.0 CRITICAL EVALUATION

4.1 Relevance of facts presented

Background information and post-accident visual inspection

Whilst any post-accident visual inspection of the accident site is generally extremely helpful in aiding any failure investigation, the addition of most figures, Figures 2, 4, 5 and 6, in Section 3 of the report are not pertinent to the subsequent analysis. The inclusion of these figures is confusing and prompts the reader the question why any other structural analysis to assess the load capacity of other silo components, such as the anchor bolts or vertical U-stiffeners, was not considered.

Similarly, information provided relating to the ventilation of the silo is not required as it is not considered in the analysis provided. Whilst stating that the silo was constructed with corrugated sheet-metal, the authors fail to take into account for this geometry in their analysis.

Tensile Testing

Although it is useful to gather tensile properties through experimentation as they provide a failure criterion for the strength analysis, results should not be used as a sole method of material identification. The steel's designation would more commonly be identified using chemical composition analysis such as optical emissions spectrometry.

Furthermore, Figure 8 in the authors' report raises questions regarding the origins and preparation of the test specimen. This figure does not clearly show the corrugated nature of the specimen nor is there a specific diagram or reference in the authors report clearly indicating the orientation of the specimen in relation to the 'main crack'. The authors should also confirm that the material was not flattened during fabrication of test specimens, as this may alter the mechanical properties.

4.2 Missing information

Metallographic Examination

The use of metallographic analysis was important to ascertain a reasonable residual wall thickness due to corrosion attack and to rule out general material failure. However both figures in the report, Figures 10 and 11, are inadequately labeled and the orientation of the samples shown is unclear. The authors fail to acknowledge the stress concentration region due to corrosion as shown in Figure 11.

Strength Analysis

A key piece of information missing from the strength analysis conducted concerns the assumed stress-state of the silo at the time of the accident. The authors are correct to assume a state of lowest static stress. However, they neglect to account for the axial compressive stress acting on the silo due to factors such as the silo's

self-weight in addition to accounting for hoop stress induced by the hydrostatic pressure of the corn. Despite this apparent omission the authors are still able to demonstrate that the sheet-metal is overloaded in corroded regions of the silo. Estimation of this compressive stress is not trivial as consideration of the geometry of the corrugations in the sheet-metal is necessary. Although this information is missing from the authors' report, we are still able to estimate axial loading acting on the silo wall using the silo design standard DIN 1055.

4.3 Appropriateness of analysis presented

Correctness and validity of the analysis presented in the article

The theoretical analysis shown in the report is arranged in a logical and rational manner. Utilizing a strength check analysis to assess whether the silo's walls were overloaded in corroded regions and a fracture mechanics method to evaluate critical crack lengths is a sound approach.

Two key comments are to be made regarding the accuracy of the analysis. The first point relates to adequately representing or describing the stress-state of the silo and the second relates to the validity of the fracture mechanics analysis method implemented.

There are two significant stress components induced on the silo wall that should be considered are:

- hoop stresses from the hydrostatic pressure of the grain
- compressive axial stresses from the silo's self-weight and wall friction effects

In general, it is important to capture the correct physics of the problem you are analyzing. Neglecting to take into account the proper geometry or incorrectly characterizing the stress-state means that you are not analyzing the problem at hand. In this instance, as confirmed in Section 3.1, the authors were correct to ignore the axial loads since they can be considered negligible, however this assumption should have been explicitly justified in their analysis. On the other hand, by neglecting the corrugation geometry the authors overestimated the hoop stresses.

With respect to the fracture mechanics analysis, the authors also correctly identified the cracking at the silo wall as a plane stress condition and correctly describe the requirements for use of linear elastic fracture mechanics (LEFM) with small-scale yielding (SSY). These requirements are:

- the size of the plastic zone \ll critical crack length
- the size of the plastic zone \ll material thickness

Whilst the authors demonstrate that the length of the plastic zone (44mm) is less than the crack length ($\approx 200\text{mm}$), the LEFM SSY method is not valid in this instance since the estimated size of the plastic zone (44mm) exceeds the silo wall thickness ($\approx 0.35\text{mm}$).

The alternative fracture mechanics approach, elastic plastic fracture mechanics (EPFM) would need to be invoked in this particular case.

Consideration of other plausible failure hypothesis

The authors, in Section 4 of their report, provide a detailed list of possible failure causes (failure hypothesis). Yet they seem to “gloss” over a rationale as to why only they consider the ‘thickness of the sheet-metal weakened by corrosion’ theory. Surely it is pertinent to justify why an analysis of stress concentrations due to the screw holes (or weakening of the screw holes) is not given further consideration given that the stress concentration factor increases three-fold when the stress concentrator is circular, according to the following equation:

$$\frac{\sigma_y}{\sigma_\infty} = \left(1 + 2\frac{c}{d}\right) = 3 \text{ when } c = d$$

This equation is based on an elliptical hole in a wide plate subjected to uniform tension [3], where σ_∞ is the far-field (applied stress).

4.4 Failure prevention

The root cause of failure is directly attributed to the corrosion of the material, namely in the thickness direction originating at an inspection window. While the authors do an adequate job of showing this, no attempt is made at identifying measures that can be taken for preventing similar occurrences. Presented below are possible changes in manufacturing and design, and inspection techniques that could prevent failure situations in similar silos.

Manufacturing and Design

Changes in the manufacturing and design of the silo could have prevented not only the corrosion but the crack propagation as well. Had more care been taken in the installation of the inspection window, the exposed edges of non-galvanized steel could have been protected with an alternative coating or sealant after the installation of the window to protect the steel from the environment. This solution

is simple and cost effective. Sealing the window would create a much lower chance of corrosion occurring but further measures can be taken to ensure a higher fracture toughness and resistance to crack propagation.

While the manufacturing process taken to create the corrugated sheet is not entirely known, it may be possible to induce a compressive residual stress in the hoop direction during manufacturing to counteract the tensile hoop stress (the leading factor in crack propagation) experienced in normal usage. Crack arresters could also be implemented into the silo design. Bands of rubber or other material could be positioned horizontally around the silo in desired locations to arrest or divert any unnoticed cracks.

Finally, if economically feasible, the silos could be created out of two or more thinner sheets of corrugated steel as opposed to one thicker sheet. This would add resistance to both crack propagation and corrosion. While one sheet may become cracked or corroded the system as a whole would not fail. All of the previously mentioned manufacturing and design changes would help prevent failure, but the simplest preventative measure may be better inspection techniques.

Inspection

As shown in the authors' analysis, the crack was substantially long and the corrosion was visibly noticeable. Had any sort of regulations been in place for regular inspection the failure would have been averted. Even a simple visual inspection of the silo would have alerted users to the corrosion. It seems very unlikely because of the origination of the corrosion and crack at an inspection window that it was never noticed. A crack having length of nearly 300 mm is could have and should have been noticed. If so, the silo could have been shut down until repairs were made. Having a standard for inspections would absolutely have prevented the failure of the silo in question and could possibly prevent future instances.

4.5 General comments

The group questions the relevance and purpose of the authors' article. Clearly, inadequate corrosion protection is a key factor in the probable cause of failure of the silo. The authors remark that they were not required to investigate what caused the corrosion or identify sources of stress concentrations due to corrosion (either due to neighboring screw holes or due to the corrosion of the sheet-metal walls). Yet this remark seems rather contradictory given that a post-accident investigation, experimental tests and theoretical analysis are conducted to support an accident failure hypothesis.

5.0 CONCLUSION

This report summarizes the critical evaluation of a corn silo burst failure analysis. The authors propose that the most plausible failure hypothesis for the silo burst is due to the development of a 'main crack' that was caused by the weakening of the accident silo's sheet-metal walls due to corrosion.

Importantly, it must be noted that the LEFM fracture mechanics analysis carried out by the authors is invalid. Despite this, the following key engineering analysis has been recreated:

- strength analysis: to determine whether the corroded sheet-metal was overloaded
- fracture mechanics (LEFM): to determine critical crack lengths in non-corroded and corroded regions of the sheet-metal

Supplementary studies were investigated in Section 3 relating to, examining the legitimacy of some assumptions implicitly made by the authors, including:

- the effect of taking into account the corrugated geometry in estimating the hydrostatic pressure induced on the silo
- the validity of neglecting the axial stress contribution in describing the stress-state of the silo at failure
- a comparison of the hydrostatic pressure of corn versus barley
- the sensitivity of dynamic fracture toughness factor on the calculated stress

Given the authors' intent, much of the information provided in Sections 2 and 3 of their report was not pertinent to the subsequent analysis provided in Section 6. Also it was not clear how the authors identified the material as St37-3N based solely on its tensile properties.

The authors make no attempt to identify what caused the corrosion of the sheet-metal or provide preventative measures to prevent similar accidents happening in future. On the other hand, we proposed the following measures:

- ensuring the proper sealing or coating of the exposed edges of the sheet-metal
- inclusion of crack-arresting features in the silo design
- introduction of a compressive residual stress during the manufacture of the corrugated sheet-metal (to relieve crack growth)
- re-thinking the silo design with respect to sheet thickness or the number of sheets used to form rings
- regular inspection to visually assess the development of corrosion and monitoring of cracks / crack growth

REFERENCES

- [1] G. Piskoty, S.A. Michel and M. Zraggen. "Bursting of a corn silo – An interdisciplinary failure analysis". Engineering Failure Analysis 12 (2005) 915-929.
- [2] DIN1055-6 Ed5, (2005-03) German Language - DESIGN LOADS FOR BUILDINGS; LOADS IN SILOS; EXPLANATIONS
- [3] MTRL585 Lecture Notes: 4. Fracture (www.vista.ubc.ca), downloaded Oct 15th 2012